Hindawi
Journal of Chemistry
Volume 2022, Article ID 8225088, 12 pages
https://doi.org/10.1155/2022/8225088

Research Article

Porous Carbons Derived from Desiliconized Rice Husk Char and Their Applications as an Adsorbent in Multivalent Ions Recycling for Spent Battery

Yating Sun, Geng Su, Zhaocai He, Yuan Wei, Jinbo Hu, Huaifei Liu, and Gonggang Liu

Hunan Province Key Laboratory of Materials Surface & Interface Science and Technology, College of Materials Science and Engineering, Central South University of Forestry and Technology, Changsha 410004, China

Correspondence should be addressed to Geng Su; sugeng199@163.com and Huaifei Liu; huaifei011@126.com

Received 17 February 2022; Revised 10 May 2022; Accepted 11 May 2022; Published 27 May 2022

Academic Editor: Jianqiang Liu

Recycling of spent lithium-ion batteries (LIBs) has attracted increasing attentions recently on account of continuous growth demand for corresponding critical metals/materials and environmental requirement of solid waste disposal. In this work, rice husk as one of the most abundant renewable fuel materials in the world was used to prepare rice husk char (RC) and applied to recycle multivalent ions in waste water from hydrometallurgical technology dispose of spent LIBs. Rice husk char with specific surface area and abundant pores was obtained via pickling and desilication process (DPRC). The structural characterization of the obtained rice husk char and its adsorption capacity for multivalent ions in recycled batteries were studied. XRD, TEM, SEM, Raman, and BET were used for the characterization of the raw and the modified samples. The results show rice husk chars after desilication has more flourishing pore structure and larger pore size about 50–60 nm. Meanwhile, after desilication, the particle size of rice husk char decreased to 31.392 μm, and the specific surface area is about 402.10 m^2/g. Its nitrogen adsorption desorption curve (BET) conforms to the type IV adsorption isotherm with H_3 hysteresis ring, indicating that the prepared rice husk char is a mesoporous material. And the adsorption capacity of optimized DPRC for Ni, Co, and Mn ions is 7.00 mg/g, 4.84 mg/g, and 2.67 mg/g, respectively. It also demonstrated a good fit in the Freundlich model for DPRC-600°C, and a possible adsorption mechanism is proposed. The study indicates biochar materials have great potential as an adsorbent to recover multivalent ions from spent batteries.

1. Introduction

With the development of social economy, the demand for lithium-ion and nickel metal hydride batteries in portable electronic equipment and electric vehicles is increasing, which brings more and more pressure to the environmental impact of solid waste treatment. The total global Li consumption amount for LIBs is estimated to 0.265 million tons by the year 2025 and will continue to amplify to 511 million tons by 2050 [1]. With the current growth rate, significant pressure is imposed on the supply side of cobalt and lithium. It is predicted that Co and Li will face a serious shortage in the foreseeable future [2]. More seriously, a large number of spent LIBs will be produced in the future. These spent batteries contain harmful electrolytes, such as organic solvents and lithium fluoride salts, which may contaminate soil and groundwater, seriously endangering human health and the ecological environment [3, 4]. In addition, high-priced metals contained in lithium ion batteries, such as lithium, cobalt, nickel, copper, and aluminum, also have good resource values [5]. Therefore, considering environmental and resource issues, effective recycling of spent lithium-ion batteries is crucial to ensure the sustainable development of the field [6–12]. Hydrometallurgy with high metal recovery, high product purity, low energy consumption, and minimal gas emissions is considered to be the most suitable technology for recovering spent LIBs [13]. The widely used hydrometallurgical methods include acid leaching, alkali leaching, solvent extraction [14], chemical precipitation [15], and adsorption [16]. Adsorbents include

activated carbon [17–19], metal-organic framework [20–26], and zeolite adsorbents [27–31]. Among them, carbon adsorption is considered as an ideal battery wastewater treatment technology due to its simple operation and low cost [32]. Besides, during hydrometallurgical technologies, low content of multivalent ions in waste water is urgent to be treated. Porous carbon with developed pore structure, large specific surface area, and rich surface functional groups has strong adsorption and removal of multivalent ions in battery wastewater [18].

Compared with coal resources, biomass resources have the advantages of large resources, wide sources, less pollution, and renewable resources [33]. Agricultural solid waste is a cheap biomass resource, which is common in all countries in the world. It can be transformed into porous carbon with excellent performance, including peanut shell [34], tea [35], cotton [36], and coconut shell [37]. Rice is the third largest food in the world after wheat and corn. The world produces 571 million tons of rice every year and 140 million tons of rice husk waste [38]. Rice husk is one of the cheapest and abundantly available biomass in which the constituents of rice husk are silica (20%), cellulose (40%), hemicellulose (20%), and lignin (20%) used for the preparation of carbon [39–44]. In recent years, surface-modified activated carbon was prepared to improve the adsorption capacity and removal efficiency of multivalent ions [45–47]. Under low temperature conditions, the chemical activation method can prepare activated carbon with abundant pore structure and low energy consumption. For example, potassium hydroxide as an activator can fully exploit the micropores of biochar [48]. Sanka et al. [49] studied the removal effect of RC on multivalent ions in industrial wastewater by carbonizing rice husk directly at different temperatures (500, 600, and 700°C). The results showed that the removal effect of Cr (65%), Fe (90%), and Pb (>90%) was the best when rice husk was carbonized at 600°C. Some studies have used hot alkali leaching to desiliconize rice husks. Studies have shown that alkali pretreatment of RC with sodium hydroxide (NaOH) with a mass ratio of 2–4% can reduce the ash content to 74–93% [50]. In addition, metal impurities in rice husks can also hinder the pore development of activated carbon. Ma et al. [51] treated rice husk with 2 mol/L hydrochloric acid for 1 h at 60°C, and more than 90% of the metal impurities could be extracted. Pickling of rice husks can also promote the dissolution of silica, increase the content of volatile matter and fixed carbon, and affect the pore structure and specific surface area of the material.

The performance of rice husk char for wastewater treatment mainly depends on the pore structure and pore size distribution of the carbon material. In addition, the high silica content in rice husk ash can also hinder the pore development of activated carbon. Therefore, the removal of silica from rice husk is an important key to the formation of porous structure. Vunain et al. [52] used rice husk as raw material and reacted potassium hydroxide with silica in rice husk to generate soluble sodium silicate for desilication, which was then activated by phosphoric acid and pyrolyzed at 600°C. By adjusting pH value, it is found that when pH value is 2.0, the adsorption capacity of Cr (VI) is the largest, and the removal rate of Cr is up to 99.88%.

In this paper, rice husk as one of the most abundant renewable fuel materials in the world was used to prepare rice husk char (RC) and applied to recycle multivalent ions in wastewater from hydrometallurgical technology dispose of spent LIBs. The pickling activated carbonized rice husk char (PRC) was desilicated by NaOH solution, which provided a new carbon material in multivalent ions recycling for spent battery and opened up a new field for the application of rice husk. The comprehensive diagram of specific routes is shown in Figure 1. The surface morphology of untreated rice husk char (RC), pickling rice husk char (PRC), and desilicated pickling rice husk char (DPRC) is analyzed, and the adsorption capacities of Co, Ni and Mn ions in spent battery wastewater by DPRC-600°C are investigated.

2. Materials and Methods

2.1. Materials. The rice husks come from Changsha suburb, the chemical reagent sodium hydroxide (NaOH, AR) comes from Shanghai Sinopharm (China), and the hydrochloric acid (HCl, 37%, AR) was purchased from Chengdu Kelong Chemical Co. (China).

2.2. Preparation of PRC and DPRC. The rice husks used in the research were taken from the suburbs of Changsha. 50-g rice husk was taken and soaked in 200 ml of 0.1 mol/L (1 : 4 solid–liquid ratio in hydrochloric acid) for 12 hours [51], then washed, dried and crushed, and passed through a gauze mesh of 100 mesh. This was then followed by the pyrolysis treatment (activation) step in which pickled rice husk powder was placed into a quartz boat for carbonization. In a nitrogen atmosphere, the temperature was increased at a rate of 10°C/min, kept at 300°C for 15 min, and then heated to 500°C and 600°C for carbonization for 3 h to prepare 500°C carbonized rice husks and 600°C carbonized rice husks, which denoted as pickled rice husk char (PRC). 10 g of PRC was weighed and mixed with 96 mL of 1 mol/L NaOH solution in a mass ratio of 1 : 10 and stirred in a constant temperature magnetic stirrer at 60°C for 6 hours [50]. The desilication solution was then vacuum filtered, while it was hot, and the precipitate was filtered, washed to nitrite at pH 7, and dried in an oven at 45°C to obtain desilication pickling rice husk char (DPRC). After adding the excess acid solution for 24 hours, the change of filtrate was observed.

2.3. Characterization of PRC and DPRC. The physicochemical characterizations of porous carbons including the morphologies, carbon structural properties, and pore structure were analyzed. The morphologies of porous carbons were characterized by scanning electron microscope (SEM, TESCAN MIRA3, Czech Republic). The carbon structural properties of porous carbons were analyzed by X-ray diffraction (XRD, Bruker D8 Advance, Germany) via Cu Kα radiation. The Raman analysis was performed in a laser Raman spectrometer (Raman, Horiba LabRAM HR Evolution, Japan). The TEM analysis was performed by a

Figure 1: Synthesis and application of DPRC.

transmission electron microscope (TEM, FEI Tecnai F20, TF30, Holland). The pore structure and the specific surface areas of porous carbons were analyzed by the nitrogen adsorption and desorption isotherm at 77 K, 1.33 Pa (BET, ASAP2010, USA). The particle size parameters of the materials were determined by Laser particle sizer (Hydro 2000Mu England). The contents of metals in the solution before and after adsorption treatment were determined by ICP-AES with inductively coupled plasma emission spectrometer (ICP, PQ9000, Germany).

2.4. Adsorption Experiments. The battery waste solution was diluted in 100 times to get solution A, and the concentrations of Ni, Co, and Mn ions in battery waste solution A are 464 g/L, 408 g/L, and 248 g/L, respectively. The battery waste solution was diluted in 2 times to get solution B.

In adsorption process, 50 mL of solution A and B was, respectively, put into two beakers, and 0.3-g rice husk activated carbon was added to each, kept at 30°C in a constant temperature magnetic stirrer, pH was adjusted to 5, stirred for 2 h, the adsorption solution was removed and filtered, and the change of adsorption solution content was analyzed. The content of multivalent ions in rice husk solution before and after porous carbon adsorption treatment was determined by ICP-AES.

3. Results and Discussion

3.1. Characterization of Samples. Figure 2 shows the typical SEM images of obtained porous carbons. It can be seen from the Figures 2(a) and 2(b) that both the pickled rice husk chars (PRC) and unpickled rice husk chars (RC) have pores, and the pore structure of the RC is not obvious. Figure 2(c) shows the diagram of rice husk carbon without acid pickling and direct desilication (DRC). The comparison result between Figures 2(c) and 2(d) shows that the pore structure distribution of DPRC is more closely distributed. Therefore, pickling treatment promotes the development of pores in rice husk char. After desilication treatment process, the Si-rich protective layer structure on the outer surfaces of PRC disappeared. The outer surface of DPRC showed a rough morphology, and part of the pore structure was exposed.

In order to investigate the effect of temperature on porous carbon, DPRC-500°C and DPRC-600°C were prepared. Figure 3 shows clearly that the surface of the PRC is relatively smooth without a large number of pores, while the surface roughness of the DPRC increases. Besides, as can be seen from the comparison between Figures 3(c) and 3(d), when the carbonization temperature was 600°C, most of the rice husk shell is peeled off, showing the internal network porous structure, and the pore size distribution is more uniform. Therefore, the carbonization temperature has a certain influence on the structure of porous carbon.

TEM characterization was conducted to further characterize the morphology of rice husk chars before and after desilication. Figure 4 shows the TEM images of PRC-600°C (Figures 4(a), 4(b)) and DPRC-600°C (Figures 4(c), 4(d)). It can be seen from Figures 4(a), 4(b), PRC-600°C has typical porous structure, and its surface pore size is about 25–30 nm. As shown in Figures 4(c), 4(d), DPRC-600°C has a looser porous structure, and the pores of the rice husk carbon material after desilication are more flourishing and obviously enlarged. The pore size is about 50–60 nm. The results indicate rice husk chars after desilication has more flourishing pore structure and larger pore size.

The colors of the desilication filtrate at different carbonization temperatures are shown in Figures 5(a) and 5(b). Its color changes with the increase of carbonization temperature. The 500°C desiliconization filtrate is light yellow, and the 600°C desiliconization filtrate is colorless and transparent. When the carbonization temperature is low, part of the tar produced during rice husk carbonization will adhere to the surface, and the viscosity of tar is high. When dissolved in sodium hydroxide solution, the solution changes from colorless to pale yellow. The adhesion of tar will reduce the specific surface area of the obtained rice husk char; that is, the effective contact area during the desiliconization reaction will decrease, thus reducing the reaction efficiency. Therefore, when the carbonization temperature is raised to 600°C, it is conducive to the further volatilization of organic matter, the pyrolysis of tar into small molecules, and the improvement of desiliconization efficiency.

Figures 5(c) and 5(d) is the solution diagram of the desiliconization filtrate treated with acid at 600°C. Some white floccules can be seen in the Figure 4(a). After standing

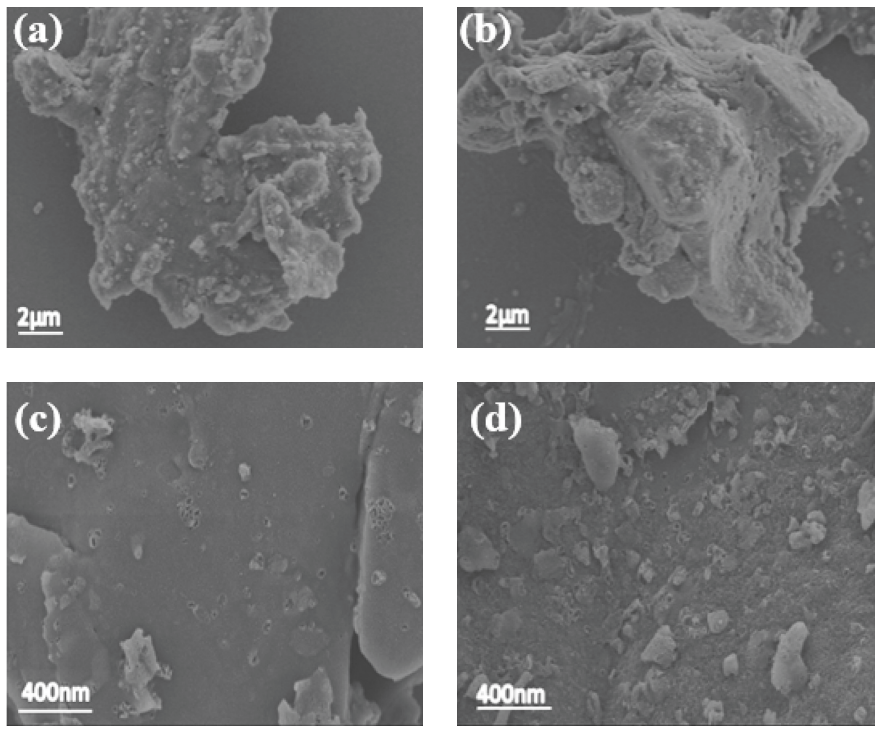

Figure 2: SEM images of RC (a) and PRC (b); SEM images of DRC (c) and DPRC (d).

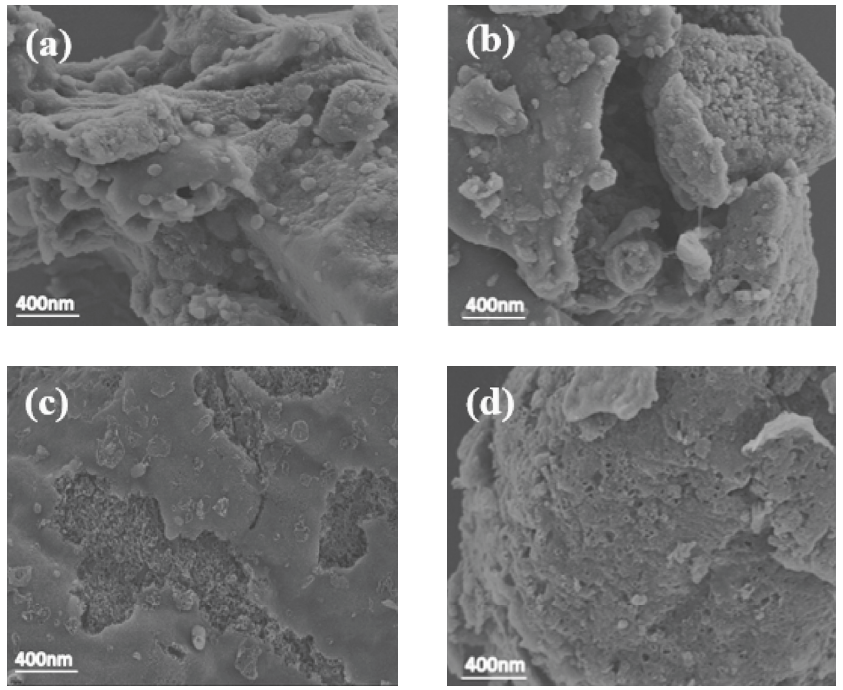

Figure 3: SEM of PRC-500°C (a) and PRC-600°C (b); SEM images of DPRC-500°C (c) and DPRC-600°C (d).

for a period of time, hydrochloric acid reacts with sodium silicate in the filtrate to form a gel, indicating that silicon dioxide dissolves from PRC during hot-base desilication. Therefore, combined with the SEM analysis, the optimum carbonization temperature of the rice husk char is 600°C.

The XRD patterns of PRC-600°C, DPRC-600°C, and DPRC-500°C are shown in Figure 6(a). All samples exhibited two typical diffraction peaks at around 22° and 45° corresponding to the diffuse reflection of amorphous nature and low graphitization degree of carbon framework. The existence of the amorphous structure may be due to the

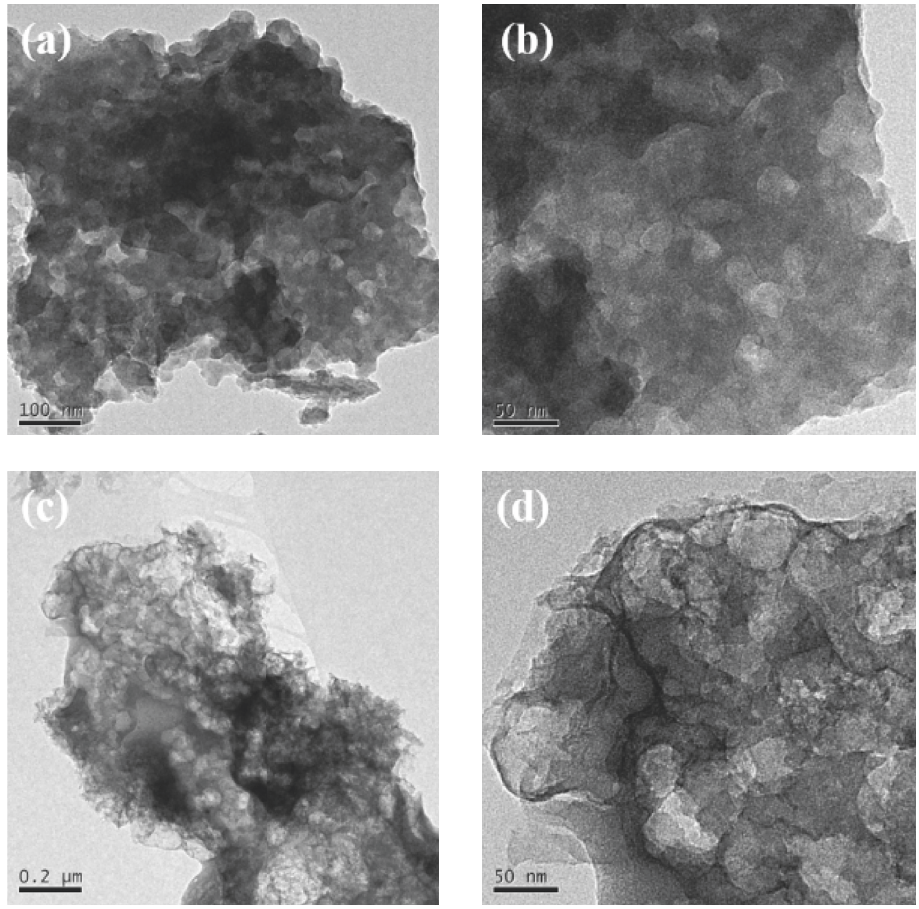

Figure 4: TEM of PRC-600°C (a), (b) and DPRC-600°C (c), (d).

diffraction overlap between the silica crystal plane and the carbon (002) crystal plane in rice husk [53].

XRD patterns also show that the DPRC-500°C and DPRC-600°C phase structures are similar. Compared with the other two curves, the diffraction peak shape of DPRC-600°C in the range of 15~30° becomes wider. This may be caused by the further decomposition of organic matter during high temperature pyrolysis, which increases the carbon disorder degree. In the process of hot NaOH treatment, the dissolution of silica will also reduce the intensity and shape of the diffraction peaks of DPRC, but the decrease is relatively low, indicating that the desiliconization is not complete. At 2θ of 45°, the intensity of the diffraction peak increases, and the peak shape becomes sharp, which indicates that the rice husk char after hot alkali treatment becomes more ordered and regular, and the degree of graphitization increases, which will lead to a decrease in the interlayer spacing of the pore structure and the decrease in the adsorption properties of the material.

The carbon crystallinity of rice husk-derived PRC and DPRC has been presented by Raman spectra as shown in Figure 6(b). The spectra of both PRC and DPRC presented two peaks at 1358 and 1591 cm^{-1}, corresponding to the characteristic D (structural defects associated with disordered carbon structure) band and G (graphite crystals associated with sp^2-ordered carbon structure) band, respectively [54]. The ratio of relative intensity of the two peaks (I_D/I_G) for PRC and DPRC was found to be 2.94 and 2.73, respectively. It indicated that the carbon composite obtained from pyrolysis of rice husk sample after NaOH desilication treatment had a higher graphitization degree. Raman results are consistent with XRD results. After desilication, rice husk carbon will form original defects and form porous structure, resulting in a large specific surface area, which is conducive to ion adsorption.

Particle size parameters of PRC and DPRC are shown in Table 1. The particle size of PRC is less than 5.965 μm; accounting for 10%, the average particle size is 45.184 μm, and 90% of the particles are less than 111.909 μm in size. The average particle size of the DPRC was 31.392 μm, and 90% of the particles were smaller than 89.619 μm. Comparing the two, it can be seen that the particle size of the DPRC has decreased. After carbonization, the epidermal cells where silica is mainly distributed in rice husk were destroyed, and the volatilization of organic matter reduced the connection degree between lignin and silica. In the process of thermo-alkali treatment, silica in rice husk is easy to react with sodium hydroxide and dissolve out, and certain pores are developed. In addition, the dissolution of silica as skeleton will lead to loose material structure, and DPRC will be more easily broken in subsequent grinding. These are the main reasons for the smaller particle size of DPRC.

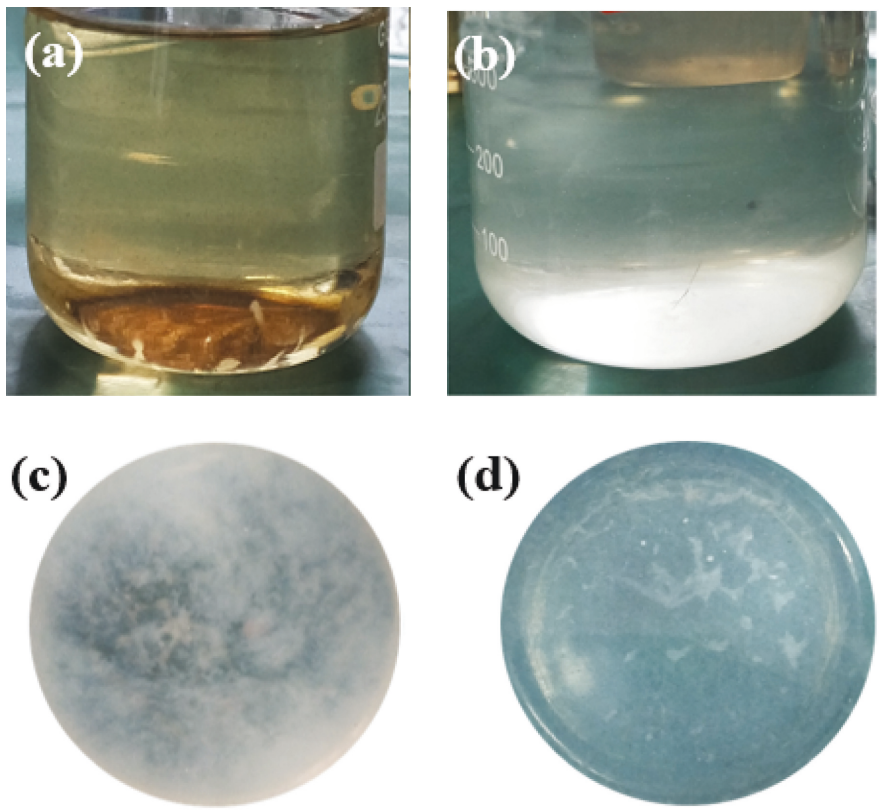

Figure 5: 500°C desiliconization filtrate (a), 600°C desiliconization filtrate (b); solution after acid treatment of desiliconization filtrate at 600°C (c) and solution after standing for 24 h (d).

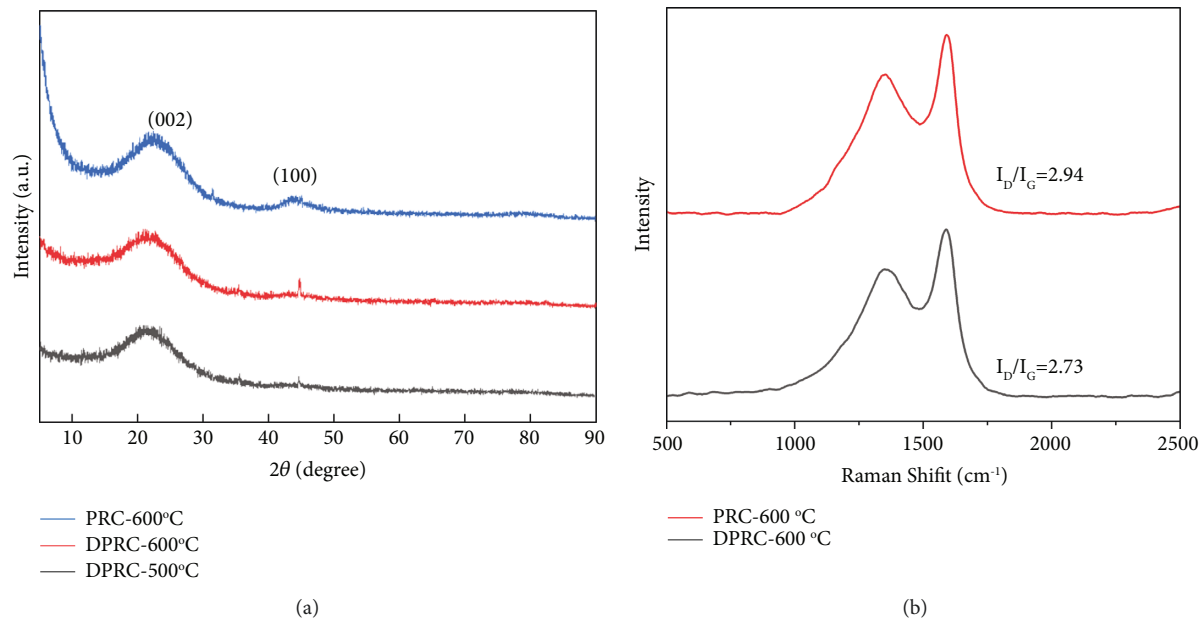

Figure 6: (a) XRD patterns of PRC-600°C, DPRC-600°C, and DPRC-500°C. (b) Raman spectra of PRC-600°C and DPRC-600°C.

Silica is mainly concentrated in the striated outer skin of rice husk, especially the raised part. After carbonization, the epidermal cells of rice husk were destroyed, and organic matter was volatilized at high temperature, which reduced the binding degree of lignin and silica. In the process of thermo-alkali treatment, silica in rice husk is easy to react with sodium hydroxide to precipitate and form certain pores. At the same time, silica acts as a skeleton, and its dissolution leads to loose structure, which explain why DPRC is more easily broken and has smaller particle size.

The pore structure and the pore size distribution of porous carbons are investigated via the N_2 adsorption/desorption

Table 1: Particle size analysis of PRC and DPRC.

Samples	PRC	DPRC
Surface area average particle size (μm)	14.447	11.840
Volume average particle size (μm)	51.993	39.919
D (0.1) (μm)	5.965	5.010
D (0.5) (μm)	45.184	31.392
D (0.9) (μm)	111.909	89.619

isotherms as illustrated in Figure 7. As seen from the Figure 7(a), the N_2 adsorbed increases sharply when the value of P/P_0 is under 0.1 and it indicates the existence of micropores. Then, with the increase of relative pressure, the adsorption capacity increases gradually. When $P/P_0 > 0.5$, there is a hysteresis loop, and the adsorption capacity of the material continues to increase with the increase of the relative pressure. When the relative pressure is 1.0, the adsorption value reaches the maximum, indicating that there is a certain amount of mesopores in the sample. The initial part of the isotherm is due to the volume filling effect of the micropores, which can complete the adsorption equilibrium in a relatively short time. However, with the increasing relative pressure, the microporous adsorption gradually transformed into mesoporous adsorption, and capillary condensation occurred in the mesopores, which increased the adsorption amount of N_2. It can be seen from the Figure 7(a) that N_2 adsorption-desorption isotherms of the two rice husk char conform to typical type IV adsorption isotherms. And PRC has H_4 hysteresis ring, while DPRC has H_3 hysteresis ring. The results show that the desilication process of rice husk char enlarged some micropores into mesopores. With the increase of mesoporous structures and mesoporous pores in the appearance, the isotherms changed accordingly [55]. Therefore, N_2 adsorption capacity of DPRC at $P/P_0 < 0.1$ microporous adsorption stage is less than that of rice husk char. As the number of mesopores increased, the maximum N_2 adsorption of DPRC was higher than that of PRC and the hysteresis ring of desilicated rice husk char appeared earlier. As it can be seen from Figure 7(b), the difference in pore structure between PRC and DPRC is mainly in the mesoporous region of 2–50 nm. DPRC has a larger internal pore size, with fewer mesopores in the range of 2–17 nm than PRC, and more pore sizes in the range of 17–50 nm. This indicates that desilication sample is a kind of mesoporous material with less micropore number, more mesoporous number, and larger mesoporous aperture than PRC, which is consistent with the isotherm analysis of nitrogen adsorption and desorption shown in Figure 7(a). The BET results are consistent with TEM observation results.

To further evaluate the impact of desilication treatment, the pore structure characteristics of PRC and DPRC are summarized in Table 2. It was found that desilication treatment increased the values of average pore size and pore volume, especially the mesoporosity. However, DPRC has a BET surface area of 402.10 m^2/g, which is slightly lower than that of PRC (470.67 m^2/g). Combined with the pore size distribution diagrams in Figure 7(b), it can be seen that the number of micropores in the DPRC decreases and the number of mesopores increases, thereby reducing the specific surface area. This phenomenon is attributable to the removal and destruction of SiO_2 protective layer of PRC, promoting the development and transformation of some micropores to mesopores [56]. In addition, most of the grain size of silica in rice husk is between 8 and 22 nm, while only a small part is between 1 and 7 nm.

3.2. Multivalent Ions Recycling for Spent Battery. SEM images show that DPRC has abundant and uniform pores. BET results show that the specific surface area is 402.10 m^2/g. As a result, DPRC is easy to form physical and chemical adsorption with multivalent ions in wastewater, which has certain adsorption and purification effects. Figure 8 show the comparison of the adsorption capacity of 0.30 g of rice husk char to treat 50 mL of high and low concentration battery wastewater. The adsorption capacity of Ni, Co, and Mn ions by DPRC in high-concentration A solution is 7.00 mg/g, 4.84 mg/g, and 2.67 mg/g, respectively. While in the low-concentration B solution, the adsorption capacity is 5.00 mg/g, 2.34 mg/g, and 1.84 mg/g, respectively. The results show that DPRC has a large adsorption capacity for A solution. This may be because the increase of metal ion concentration increases the probability of ion contact collision with DPRC adsorption site of rice husk. Therefore, the filling rate of DPRC adsorption site by ion adsorption material is increased, and the adsorption capacity of the material is increased. At the same time, the adsorption capacity of Ni on the DPRC is the largest, followed by Co and Mn. The reason for this phenomenon may be that the competitive adsorption of multivalent ions and the adsorption of Co and Mn on DPRC are affected by the saturated adsorption of Ni. On the other hand, the maximum adsorption capacity of different types of biochar for various multivalent metals in water is compared and shown in Table 3. From the results of reference [54–59], as-prepared DPRC has a satisfying multivalent metals adsorption capacity.

3.3. Adsorption Isotherms. The adsorption isotherms were performed with different initial concentrations ranging from 40 to 900 mg/L, at optimized pH of 5. The adsorbent dose is 300 mg with constant agitation at a fixed duration of 120 min. Different initial concentrations of wastewater were prepared by proper dilution of 105.92 g/L battery wastewater with distilled water, and the results are presented in Figure 9. With an increase of total concentration of Ni, Co, and Mn ions from 40 to 900 mg/L, the equilibrium adsorption capacity of Ni, Co, and Mn ions has increased from 2.96 to 14.5 mg/g. It has been established that as the initial concentration of Ni, Co, and Mn ion solution increased, the amount of these ions adsorbed per unit mass of the adsorbents has a substantial increase. It may be because the rate of adsorption occurred at reduced pace but increasing the concentration resulting in the competition of binding sites on the adsorbents by ions, thereby increasing adsorption capacity at lower initial metal ion concentration [63]. Then, it has a smaller increase at higher concentration, which is due to the saturation of binding sites. This occurs due to an

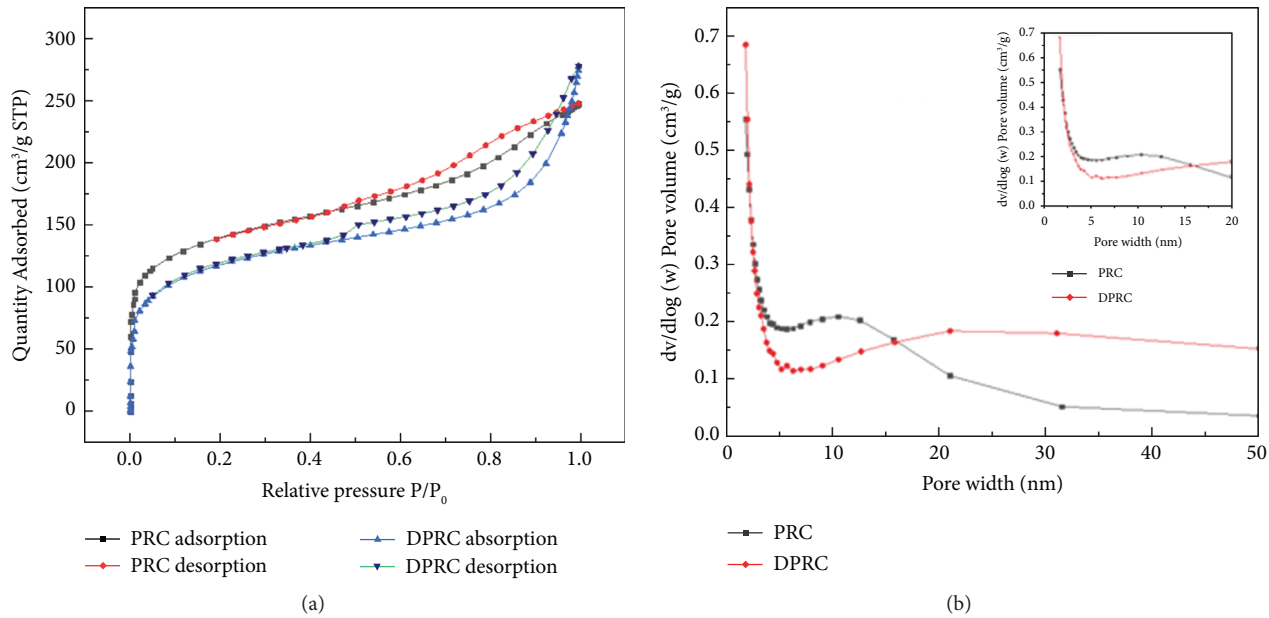

Figure 7: Nitrogen adsorption-desorption isotherms of PRC and DPRC (a); BJH pore size distribution of PRC and DPRC (b).

Table 2: Void correlation coefficient of PRC and DPRC.

Parameters	PRC	DPRC
BET specific surface area (m^2/g)	470.669	402.092
Pore volume (cm^3/g)	0.381	0.410
Average pore size (nm)	3.240	4.077
Mesopore average pore size (nm)	4.077	5.168
Average pore size of micropores (nm)	1.018	1.019

Table 3: Maximum adsorption capacities of different types of biochar to different multivalent metal ions according to references [54–59].

Material type	Adsorption capacity (mg/g) to multivalent metal ions		
Hardwood	6.79 Cu (II)	4.54 Zn (II)	[57]
Corn cob	17.21 Cd (II)		[58]
Mushroom-stick biochar	21.0 Pb (II)	9.80 Ni (II)	[59]
Rice straw	10.10 Cr (VI)		[60]
Sawdust biochar	15.10 Cu (II)		[61]
Peanut shells biochar	4.00 Cd (II)	22.82 Pb (II)	[62]

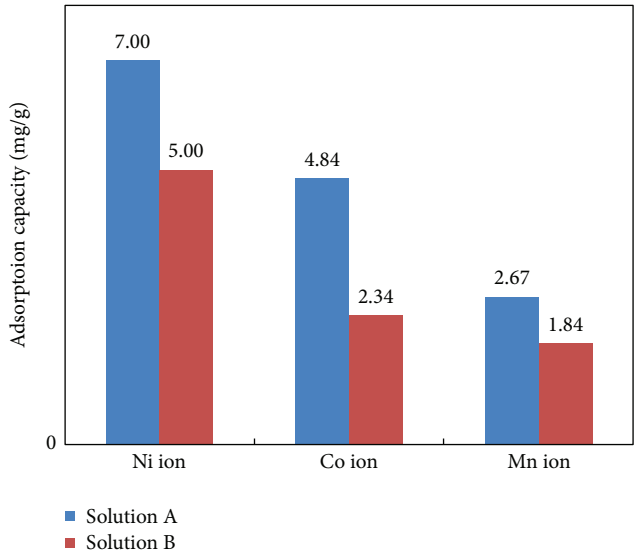

Figure 8: Ions adsorption capacity of DPRC.

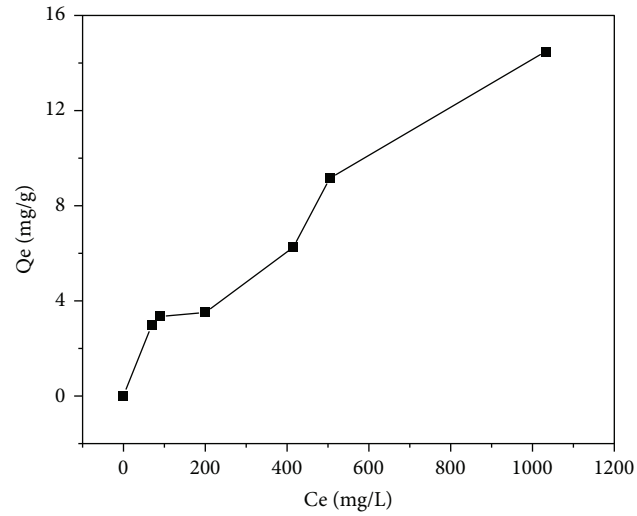

Figure 9: Absorption capacity of concentration of different initial Ni, Co, and Mn ions by DPRC-600°C.

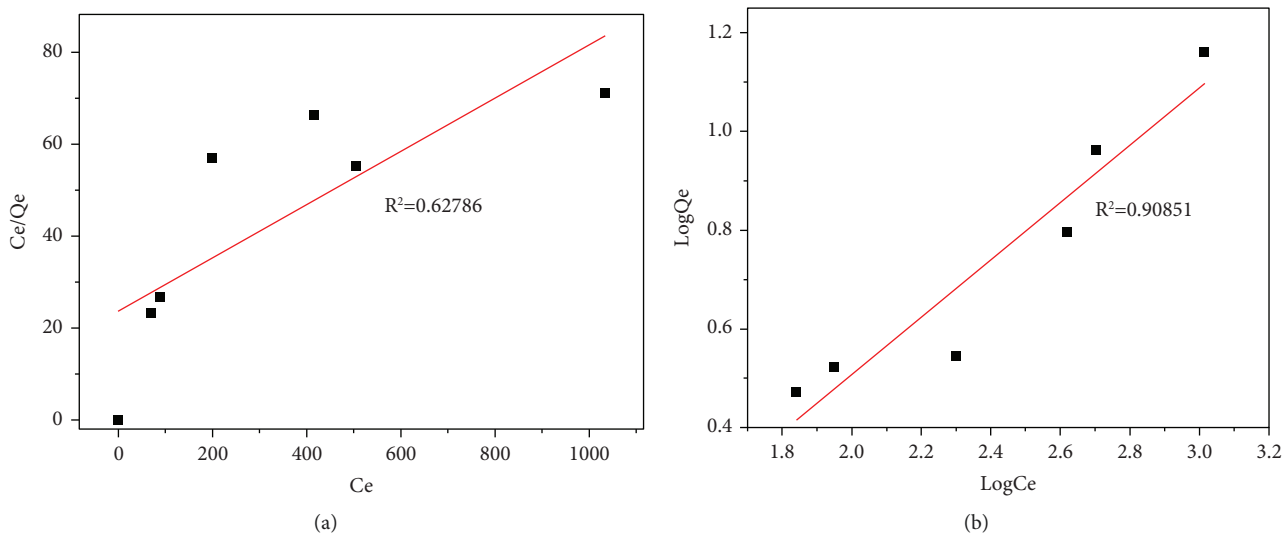

Figure 10: Langmuir plot (a) and Freundlich plot (b) for Ni, Co, and Mn adsorption on DPRC-600°C.

Table 4: Isotherm constant for the adsorption of Ni, Co, and Mn ions by DPRC-600°C.

	Langmuir			Freundlich		
	q_m	K_L	R^2	K_f	n	R^2
DPRC-600°C	17.2592	0.0245	0.6279	0.2230	1.7235	0.9085

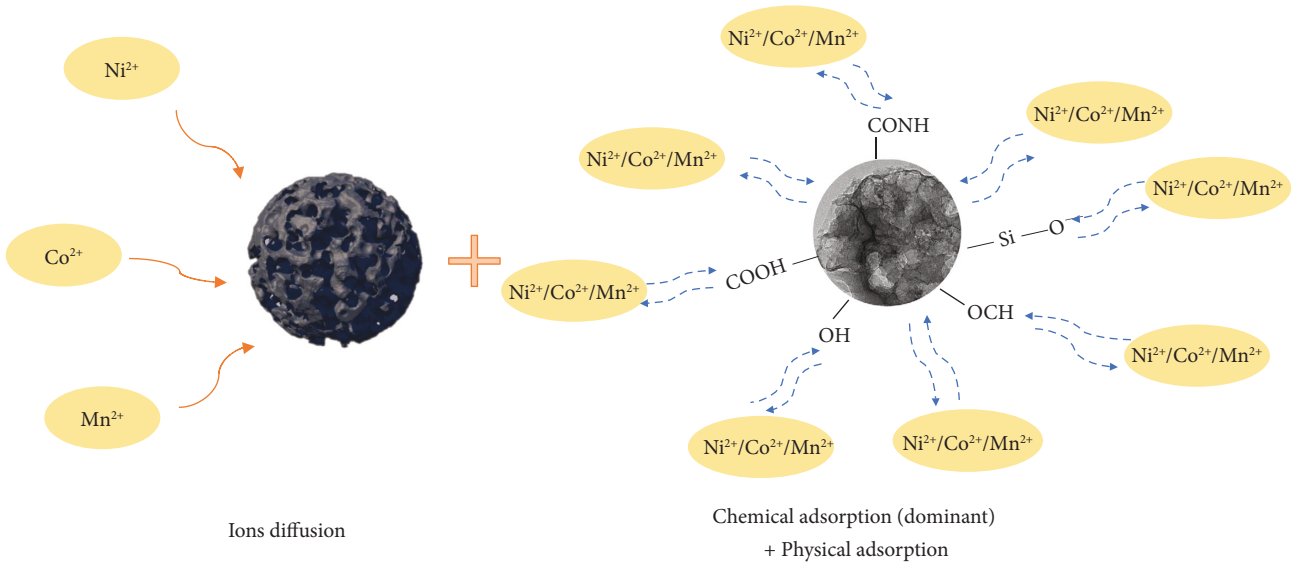

Figure 11: Possible adsorption mechanism of Ni, Co, and Mn ions on the DPRC surface.

increase in a number of ions competing for existing binding sites in the adsorbents [64].

In order to study the adsorption mechanism of DPRC for Ni, Co, and Mn ions, the adsorption isotherms were fitted with Langmuir and Freundlich models, respectively.

3.4. Langmuir Isotherm. The linearized form of this isotherm model can be represented as follows:

$$\frac{Ce}{qe} = \frac{1}{KLqm} + \frac{Ce}{qm}. \quad (1)$$

3.5. Freundlich Isotherm. The heterogeneous sorption linear model of Freundlich isotherm is expressed by the following relationship:

$$\log q_e = \log K_f + \frac{1}{n}\log C_e. \quad (2)$$

The correlation coefficient (R^2) obtained from the linear plot of Langmuir isotherm model (Figure 10(a)) for the study is 0.62786. And the correlation coefficient (R^2) obtained from the linear plot of Freundlich isotherm model (Figure 10(b)) for the study is 0.90851. It demonstrated a good fit in the Freundlich model for DPRC-600°C rather than the Langmuir isotherm model. As shown in Table 4, according to literature reports for Freundlich model [65], when the value of $1/n = 1$, the adsorption is linear. When the value of $1/n < 1$, it indicates that chemical action exists in the adsorption process. When the value is close to 0, the adsorbent is heterogeneous surface. Because the value of n is greater than 1, that is, $1/n$ is less than 1 (0.5802), the adsorption of the three multivalent ions on DPRC-600°C is heterogeneous and there is a chemical mechanism in the adsorption process [31, 65].

Based on analysis above and references [63–65], a possible adsorption mechanism of Ni, Co, and Mn ions on the DPRC surface is proposed and shown in Figure 11. After desilication treatment, the pore of rice husk carbon becomes larger, which is conducive to the diffusion of ions and subsequent adsorption. In addition to physical adsorption from these pores, there is chemical adsorption according to the model fitting results, which play an important role in adsorption process. The oxygen-containing functional groups such as hydroxyl, carbonyl, and carboxyl on the surface of DPRC-600°C can be used as adsorption sites for multivalent ions. The isolated pairs of electrons on oxygen atoms in these oxygen-containing functional groups cobond with the external orbitals of multivalent metal ions to form stable complexes to fix multivalent ions [66]. According to metal ion classification, hard metal ions (Co^{2+}, Ni^{2+}, and Mn^{2+}) are adsorbed to the surface of the oxygen-containing functional group (carboxyl and hydroxyl) [67]. In addition, a small amount of silicon-oxygen bonds may exist on the surface of DPRC-600°C though desilication process has been completed, which is also contributed to the adsorption of positive metal ions [68]. Therefore, DPRC has decent adsorption ability for Co^{2+}, Ni^{2+}, and Mn^{2+}, which may be used as an adsorbent to recover multivalent ions from spent batteries.

4. Conclusion

In this study, the facile desilication and activation route showed great ease in raise the porosity of porous carbons derived from a green and sustainable feedstock of rice husk char for recycling multivalent ions in spent battery. Rice husk biochars are prepared at different pyrolysis temperatures, that is, 500 and 600. The effects of different carbonization temperatures and desiliconization processes on the development of material pores are investigated through experiments, and their treatment effects in batteries wastewater are studied. The results show that rice husk char at the carbonization temperature of 600°C after pickling and desilication has abundant pores and uniform pore size distribution. The silica in rice husk char is dissolved after thermal alkali treatment, and the greatly increased porosity leads to a large increase in the adsorption rate of multivalent ions. Desilicated pickling rice husk char as adsorbent has potential application prospect in multivalent ions recovery of spent batteries.

Data Availability

Data sharing is not applicable to this article as no new data were created or analyzed in this study.

Conflicts of Interest

The authors declare that they have no conflicts of interest.

Acknowledgments

This work was supported by the Scientific Research Project of Hunan Education Department (21B0242), Hunan Provincial Natural Science Foundation of China (2020JJ5962, 2020JJ2058, and 2019JJ40535), and Hunan high-level talent gathering project-innovative talents (No. 2019RS1061).

References

[1] S. Yang, F. Zhang, H. Ding, P. He, and H. Zhou, "Lithium metal extraction from seawater," *Joule*, vol. 2, no. 9, pp. 1648–1651, 2018.

[2] W. Lv, Z. Wang, H. Cao, Y. Sun, Y. Zhang, and Z. Sun, "A critical review and analysis on the recycling of spent lithium-ion batteries," *ACS Sustainable Chemistry & Engineering*, vol. 6, no. 2, pp. 1504–1521, 2018.

[3] J. B. Goodenough and K.-S. Park, "The Li-ion rechargeable battery: a perspective," *Journal of the American Chemical Society*, vol. 135, no. 4, pp. 1167–1176, 2013.

[4] M. Chen, X. Ma, B. Chen et al., "Recycling end-of-life electric vehicle lithium-ion batteries," *Joule*, vol. 3, no. 11, pp. 2622–2646, 2019.

[5] L.-F. Zhou, D. Yang, T. Du, H. Gong, and W. B. Luo, "The current process for the recycling of spent lithium ion batteries," *Frontiers of Chemistry*, vol. 8, 2020.

[6] R. E. Ciez and J. F. Whitacre, "Examining different recycling processes for lithium-ion batteries," *Nature Sustainability*, vol. 2, no. 2, pp. 148–156, 2019.

[7] Y. Zhao, X. Yuan, L. Jiang et al., "Regeneration and reutilization of cathode materials from spent lithium-ion batteries," *Chemical Engineering Journal*, vol. 383, Article ID 123089, 2020.

[8] J. Xiao, J. Li, and Z. Xu, "Challenges to future development of spent lithium ion batteries recovery from environmental and technological perspectives," *Environmental Science & Technology*, vol. 54, no. 1, pp. 9–25, 2019.

[9] F. Arshad, L. Li, K. Amin et al., "A comprehensive review of the advancement in recycling the anode and electrolyte from spent lithium ion batteries," *ACS Sustainable Chemistry & Engineering*, vol. 8, no. 36, pp. 13527–13554, 2020.

[10] S. A. El-Safty, M. Awual, M. Shenashen, and A. Shahat, "Simultaneous optical detection and extraction of cobalt (II) from lithium ion batteries using nanocollector monoliths," *Sensors and Actuators B: Chemical*, vol. 176, pp. 1015–1025, 2013.

[11] D. J. Garole, R. Hossain, V. J. Garole, V. Sahajwalla, J. Nerkar, and D. P. Dubal, "Recycle, recover and repurpose strategy of

spent li-ion Batteries and catalysts: current status and future opportunities," *ChemSusChem*, vol. 13, no. 12, pp. 3079–3100, 2020.

[12] D. L. Thompson, J. M. Hartley, S. M. Lambert et al., "The importance of design in lithium ion battery recycling-a critical review," *Green Chemistry*, vol. 22, no. 22, pp. 7585–7603, 2020.

[13] Y. Yao, M. Zhu, Z. Zhao, B. Tong, Y. Fan, and Z. Hua, "Hydrometallurgical processes for recycling spent lithium-ion batteries: a critical review," *ACS Sustainable Chemistry & Engineering*, vol. 6, no. 11, pp. 13611–13627, 2018.

[14] G. Hu, J. Li, and H. Hou, "A combination of solvent extraction and freeze thaw for oil recovery from petroleum refinery wastewater treatment pond sludge," *Journal of Hazardous Materials*, vol. 283, pp. 832–840, 2015.

[15] B. P. Espósito, S. Epsztejn, W. Breuer, and Z. Cabantchik, "A review of fluorescence methods for assessing labile iron in cells and biological fluids," *Analytical Biochemistry*, vol. 304, no. 1, pp. 1–18, 2002.

[16] J. Dasgupta, D. Mondal, S. Chakraborty, J. Sikder, S. Curcio, and H. Arafat, "Nanofiltration based water reclamation from tannery effluent following coagulation pretreatment," *Ecotoxicology and Environmental Safety*, vol. 121, pp. 22–30, 2015.

[17] R. Shahrokhi-Shahraki, C. Benally, M. G. El-Din, and J. Park, "High efficiency removal of heavy metals using tire-derived activated carbon vs. commercial activated carbon: insights into the adsorption mechanisms," *Chemosphere*, vol. 264, Article ID 128455, 2021.

[18] D. Kołodyńska, J. Krukowska, and P. Thomas, "Comparison of sorption and desorption studies of heavy metal ions from biochar and commercial active carbon," *Chemical Engineering Journal*, vol. 307, pp. 353–363, 2017.

[19] M. Safa Gamal, N. Asikin-Mijan, M. Arumugam, U. Rashid, and Y. Taufiq-Yap, "Solvent-free catalytic deoxygenation of palm fatty acid distillate over cobalt and manganese supported on activated carbon originating from waste coconut shell," *Journal of Analytical and Applied Pyrolysis*, vol. 144, Article ID 104690, 2019.

[20] L. Esrafili, F. D. Firuzabadi, A. Morsali, and M. L. Hu, "Reuse of predesigned dual-functional metal organic frameworks (DF-MOFs) after heavy metal removal," *Journal of Hazardous Materials*, vol. 403, Article ID 123696, 2021.

[21] N. Abdollahi, S. A. Akbar Razavi, A. Morsali, and M. L. Hu, "High capacity Hg (II) and Pb (II) removal using MOF-based nanocomposite: cooperative effects of pore functionalization and surface-charge modulation," *Journal of Hazardous Materials*, vol. 387, Article ID 121667, 2020.

[22] L. Esrafili, A. Morsali, M. L. Hu et al., "Size-selective urea-containing metal–organic frameworks as receptors for anions," *Inorganic Chemistry*, vol. 59, no. 22, pp. 16421–16429, 2020.

[23] J. Q. Liu, G. P. Li, W. C. Liu et al., "Two unusual nanocage-based ln-MOFs with triazole sites: highly fluorescent sensing for Fe^{3+} and Cr_2O7^{2-}, and selective CO_2 capture," *ChemPlusChem*, vol. 81, no. 12, pp. 1299–1304, 2016.

[24] H.-R. Fu, Y. Zhao, Z. Zhou, X. G. Yang, and L. F. Ma, "Neutral ligand TIPA-based two 2D metal–organic frameworks: ultrahigh selectivity of C_2H_2/CH_4 and efficient sensing and sorption of Cr (VI)," *Dalton Transactions*, vol. 47, no. 11, pp. 3725–3732, 2018.

[25] G.-X. Wen, M. L. Han, X. Q. Wu et al., "A multi-responsive luminescent sensor based on a super-stable sandwich-type terbium (III)–organic framework," *Dalton Transactions*, vol. 45, no. 39, pp. 15492–15499, 2016.

[26] H.-R. Fu, N. Wang, J. H. Qin, M. L. Han, L. F. Ma, and F. Wang, "Spatial confinement of a cationic MOF: a SC–SC approach for high capacity Cr (VI)-oxyanion capture in aqueous solution," *Chemical Communications*, vol. 54, no. 82, pp. 11645–11648, 2018.

[27] T. Tamiji and A. Nezamzadeh-Ejhieh, "Sensitive voltammetric determination of bromate by using ion-exchange property of a Sn (II)-clinoptilolite-modified carbon paste electrode," *Journal of Solid State Electrochemistry*, vol. 23, no. 1, pp. 143–157, 2019.

[28] M. Nosuhi and A. Nezamzadeh-Ejhieh, "An indirect application aspect of zeolite modified electrodes for voltammetric determination of iodate," *Journal of Electroanalytical Chemistry*, vol. 810, pp. 119–128, 2018.

[29] M. Borandegi and A. Nezamzadeh-Ejhieh, "Enhanced removal efficiency of clinoptilolite nano-particles toward Co (II) from aqueous solution by modification with glutamic acid," *Colloids and Surfaces A: Physicochemical and Engineering Aspects*, vol. 479, pp. 35–45, 2015.

[30] S. Haghshenas and A. Nezamzadeh-Ejhieh, "Clinoptilolite nanoparticles modified with dimethyl glyoxime as a sensitive modifier for a carbon paste electrode in the voltammetric determination of Ni (II): experimental design by response surface methodology," *New Journal of Chemistry*, vol. 41, no. 22, pp. 13355–13364, 2017.

[31] A. Nezamzadeh-Ejhieh and M. Kabiri-Samani, "Effective removal of Ni (II) from aqueous solutions by modification of nano particles of clinoptilolite with dimethylglyoxime," *Journal of Hazardous Materials*, vol. 260, pp. 339–349, 2013.

[32] A. Mullick, S. Moulik, and S. Bhattacharjee, "Removal of hexavalent chromium from aqueous solutions by low-cost rice husk-based activated carbon: kinetic and thermodynamic studies," *Indian Chemical Engineer*, vol. 60, no. 1, pp. 58–71, 2018.

[33] S. De, A. M. Balu, J. C. van der Waal, and R. Luque, "Biomass-derived porous carbon materials: synthesis and catalytic applications," *ChemCatChem*, vol. 7, no. 11, pp. 1608–1629, 2015.

[34] L. A. d. Silva, S. M. S. Borges, P. N. Paulino et al., "Methylene blue oxidation over iron oxide supported on activated carbon derived from peanut hulls," *Catalysis Today*, vol. 289, pp. 237–248, 2017.

[35] Z. Guo, Z. Xiao, G. Ren et al., "Natural tea-leaf-derived, ternary-doped 3D porous carbon as a high-performance electrocatalyst for the oxygen reduction reaction," *Nano Research*, vol. 9, no. 5, pp. 1244–1255, 2016.

[36] X. Duan, C. Srinivasakannan, X. Wang, F. Wang, and X. Liu, "Synthesis of activated carbon fibers from cotton by microwave induced H3PO4 activation," *Journal of the Taiwan Institute of Chemical Engineers*, vol. 70, pp. 374–381, 2017.

[37] Q. Liang, Y. Liu, M. Chen et al., "Optimized preparation of activated carbon from coconut shell and municipal sludge," *Materials Chemistry and Physics*, vol. 241, Article ID 122327, 2020.

[38] M. M. Alam, M. A. Hossain, M. D. Hossain et al., "The potentiality of rice husk-derived activated carbon: from synthesis to application," *Processes*, vol. 8, no. 2, p. 203, 2020.

[39] E. I. El-Shafey, "Behaviour of reduction–sorption of chromium (VI) from an aqueous solution on a modified sorbent from rice husk," *Water, Air, and Soil Pollution*, vol. 163, no. 1-4, pp. 81–102, 2005.

[40] H. Jaman, D. Chakraborty, and P. Saha, "A study of the thermodynamics and kinetics of copper adsorption using chemically modified rice husk," *Clean—Soil, Air, Water*, vol. 37, no. 9, pp. 704–711, 2009.

[41] N. Yalçın and V. Sevinç, "Studies of the surface area and porosity of activated carbons prepared from rice husks," *Carbon*, vol. 38, no. 14, pp. 1943–1945, 2000.

[42] Y. Guo, S. Yang, K. Yu, J. Zhao, Z. Wang, and H. Xu, "The preparation and mechanism studies of rice husk based porous carbon," *Materials Chemistry and Physics*, vol. 74, no. 3, pp. 320–323, 2002.

[43] Y. Guo, K. Yu, Z. Wang, and H. Xu, "Effects of activation conditions on preparation of porous carbon from rice husk," *Carbon*, vol. 41, no. 8, pp. 1645–1648, 2003.

[44] A. K. Rout and A. Satapathy, "Study on mechanical and tribo-performance of rice-husk filled glass–epoxy hybrid composites," *Materials & Design*, vol. 41, pp. 131–141, 2012.

[45] O. Amuda, A. Giwa, and I. Bello, "Removal of heavy metal from industrial wastewater using modified activated coconut shell carbon," *Biochemical Engineering Journal*, vol. 36, no. 2, pp. 174–181, 2007.

[46] S. Maghsoodloo, B. Noroozi, A. Haghi, and G. Sorial, "Consequence of chitosan treating on the adsorption of humic acid by granular activated carbon," *Journal of Hazardous Materials*, vol. 191, no. 1-3, pp. 380–387, 2011.

[47] M. Hasan, A. Ahmad, and B. Hameed, "Adsorption of reactive dye onto cross-linked chitosan/oil palm ash composite beads," *Chemical Engineering Journal*, vol. 136, no. 2-3, pp. 164–172, 2008.

[48] K. Yang, L. Zhu, J. Yang, and D. Lin, "Adsorption and correlations of selected aromatic compounds on a KOH-activated carbon with large surface area," *The Science of the Total Environment*, vol. 618, pp. 1677–1684, 2018.

[49] P. M. Sanka, M. J. Rwiza, and K. M. Mtei, "Removal of selected heavy metal ions from industrial wastewater using rice and corn husk biochar," *Water, Air, & Soil Pollution*, vol. 231, no. 5, pp. 244–313, 2020.

[50] E. Menya, P. Olupot, H. Storz, M. Lubwama, and Y. Kiros, "Production and performance of activated carbon from rice husks for removal of natural organic matter from water: a review," *Chemical Engineering Research and Design*, vol. 129, pp. 271–296, 2018.

[51] Y. Ma, H. Zhang, H. Yang, and Y. Zhang, "The effect of acid washing pretreatment on bio-oil production in fast pyrolysis of rice husk," *Cellulose*, vol. 26, no. 15, pp. 8465–8474, 2019.

[52] E. Vunain, D. Kenneth, and T. Biswick, "Synthesis and characterization of low-cost activated carbon prepared from Malawian baobab fruit shells by H3PO4 activation for removal of Cu (II) ions: equilibrium and kinetics studies," *Applied Water Science*, vol. 7, no. 8, pp. 4301–4319, 2017.

[53] J.-H. Lee, Y.-J. Heo, and S.-J. Park, "Effect of silica removal and steam activation on extra-porous activated carbons from rice husks for methane storage," *International Journal of Hydrogen Energy*, vol. 43, no. 49, pp. 22377–22384, 2018.

[54] X. Zhu, Y. Liu, G. Luo, F. Qian, S. Zhang, and J. Chen, "Facile fabrication of magnetic carbon composites from hydrochar via simultaneous activation and magnetization for triclosan adsorption," *Environmental Science & Technology*, vol. 48, no. 10, pp. 5840–5848, 2014.

[55] R.-L. Tseng, "Mesopore control of high surface area NaOH-activated carbon," *Journal of Colloid and Interface Science*, vol. 303, no. 2, pp. 494–502, 2006.

[56] B. Xue, L. Jin, Z. Chen et al., "The template effect of silica in rice husk for efficient synthesis of the activated carbon based electrode material," *Journal of Alloys and Compounds*, vol. 789, pp. 777–784, 2019.

[57] X. Chen, G. Chen, L. Chen et al., "Adsorption of copper and zinc by biochars produced from pyrolysis of hardwood and corn straw in aqueous solution," *Bioresource Technology*, vol. 102, no. 19, pp. 8877–8884, 2011.

[58] M. Moyo, S. T. Lindiwe, E. Sebata, B. C. Nyamunda, and U. Guyo, "Equilibrium, kinetic, and thermodynamic studies on biosorption of cd (II) from aqueous solution by biochar," *Research on Chemical Intermediates*, vol. 42, no. 2, pp. 1349–1362, 2016.

[59] X. Wang, X. Li, G. Liu et al., "Mixed heavy metal removal from wastewater by using discarded mushroom-stick biochar: adsorption properties and mechanisms," *Environmental Sciences: Processes & Impacts*, vol. 21, no. 3, pp. 584–592, 2019.

[60] S. Yuan, M. Hong, H. Li et al., "Contributions and mechanisms of components in modified biochar to adsorb cadmium in aqueous solution," *The Science of the Total Environment*, vol. 733, Article ID 139320, 2020.

[61] G.-X. Yang and H. Jiang, "Amino modification of biochar for enhanced adsorption of copper ions from synthetic wastewater," *Water Research*, vol. 48, pp. 396–405, 2014.

[62] Y. Xue, B. Gao, Y. Yao et al., "Hydrogen peroxide modification enhances the ability of biochar (hydrochar) produced from hydrothermal carbonization of peanut hull to remove aqueous heavy metals: batch and column tests," *Chemical Engineering Journal*, vol. 200-202, pp. 673–680, 2012.

[63] T. Dula, K. Siraj, and S. A. Kitte, "Adsorption of hexavalent chromium from aqueous solution using chemically activated carbon prepared from locally available waste of bamboo (oxytenanthera abyssinica)," *ISRN Environmental Chemistry*, vol. 2014, Article ID 438245, 9 pages, 2014.

[64] A. Murugesan, T. Vidhyadevi, S. D. Kirupha, L. Ravikumar, and S. Sivanesan, "Removal of chromium (VI) from aqueous solution using chemically modified corncorb-activated carbon: equilibrium and kinetic studies," *Environmental Progress & Sustainable Energy*, vol. 32, no. 3, pp. 673–680, 2013.

[65] B. Kayranli, "Adsorption of textile dyes onto iron based waterworks sludge from aqueous solution; isotherm, kinetic and thermodynamic study," *Chemical Engineering Journal*, vol. 173, no. 3, pp. 782–791, 2011.

[66] B. Qiu, X. Tao, H. Wang, W. Li, X. Ding, and H. Chu, "Biochar as a low-cost adsorbent for aqueous heavy metal removal: a review," *Journal of Analytical and Applied Pyrolysis*, vol. 155, Article ID 105081, 2021.

[67] A. Alfarra, E. Frackowiak, and F. Béguin, "The HSAB concept as a means to interpret the adsorption of metal ions onto activated carbons," *Applied Surface Science*, vol. 228, no. 1-4, pp. 84–92, 2004.

[68] G. Liu, S. Gui, H. Zhou, F. Zeng, Y. Zhou, and H. Ye, "A strong adsorbent for Cu^{2+}: graphene oxide modified with triethanolamine," *Dalton Transactions*, vol. 43, no. 19, pp. 6977–6980, 2014.